Hidden Horizons in Non-relativistic AdS/CFT with Fermions

Youngshin Kim

A senior thesis submitted to the faculty of
University of Michigan
in partial fulfillment of the requirements for the Honors degree of

Bachelor of Science

Professor James T. Liu, Advisor

Department of Physics

University of Michigan

March 2015

ABSTRACT

Hidden Horizons in Non-relativistic AdS/CFT with Fermions

Youngshin Kim
Department of Physics, University of Michigan
Bachelor of Science

There has been much interest in the Lifshitz spacetime as a possible holographic dual of field theories without Lorentz invariance. It has been shown that the holographic Green's function from the pure Lifshitz spacetime with bosons exhibits exponential insensitivity to the horizon boundary condition in the low energy, large momentum limit. This posed the interesting question whether the same pattern persists in AdS/CFT with fermions, which is more relavent to realistic condensed matter systems.

In this thesis, we show numerically that the same exponential suppression occurs in the fermionic Green's function constructed from the pure Lifshitz background ($z = 2, 3, 4$). In particular, we found that the exponential factors calculated from the WKB approximation in the bosonic theory carries over to the fermionic theory, with the additional factor of 2. This thesis includes a review of calculating the Green's function with the bosonic AdS/CFT prescription in the pure AdS and Lifshitz spacetime, and the useful techniques therein including the analytic method, WKB approximation, and numerical method.

Keywords: AdS/CFT, Green's function, Lifshitz, Fermion

ACKNOWLEDGMENTS

I would like to thank Professor James Liu for introducing this interesting subject to me, and teaching me a great deal of physics and mathematics, by which I have been able to make progress. I'm also very grateful for his academic guidance and warm support, which has been very valuable and will be so in my pursuit of physics.

Contents

List of Figures

List of Tables

Chapter 1

Introduction

1.1 The AdS/CFT correspondence

According to black hole thermodynamics, the entropy of black hole is proportional to the area of its horizon [1]. This idea inspired the holographic principle, which states that a region with boundary of area A is fully described by no more than A/4 degrees of freedom, or about 1 bit of information per Plank area [2].

The most explicit realization of this principle is the AdS/CFT correspondence [3]. The AdS/CFT correspondence originated from superstring theory, which unify four fundamental forces in nature, the gravity, electromagnetic force, weak force, and strong force. The correspondence claims that the two theories, 4-dimensional gauge theory and 5-dimensional gravitational theory in the AdS spacetime (the anti-de Sitter spacetime) are equivalent.

The AdS spacetime is a spacetime with a negative curvature, analgous to hyperbolic spaces. It is a vacuum solution of Einstein equation, and the opposite of de Sitter spacetime, which has a constant curvature, analogous to elliptical spaces. The AdS spacetime has a notion of boundary, and the gauge theory is called the boundary theory, while a gravitational theory is called the bulk theory.

A conformal field theory, or CFT, is a theory that has conformal symmetry. In AdS/CFT, a supersymmetric gauge theory has been typically considered, whose simplest example is the N=4 supersymmetric Yang-Mills theory. This theory has no dimensionful parameter, so has scale invariance. It also possesses conformal symmetry, which contains the Poincaré group and scale invariance. For this reason, the correspondence is called AdS/CFT.

The AdS/CFT duality is interesting in its own right, but it also has a practical importance. While gauge theory describes all forces except gravity, it is not easy to calculate a gauge theory when the coupling is strong. The duality states that one theory is strongly-coupled when the other is weakly coupled. Therefore one can analyze a strongly coupled gauge theory via a gravitational theory in the AdS spacetime with a small curvature.

In the gravitational theory, it is known that a black hole is endowed with entropy and temperature, due to the Hawking radiation. Therefore, a strongly-coupled gauge theory at finite temperature is equivalent to the gravitational theory in an AdS black hole blackground. In addition, a strongly-coupled guage theory at zero temperature is equivalent to a gravitational theory in the pure AdS spacetime, which we focus on in this thesis.

Recently, interest in applying the AdS/CFT duality to theories without Lorentz invariance has been growing, due to its relevance to condensed matter systems (see, e.g., [4; 5; 6; 7]). It is hoped that the AdS/CFT duality can provide insight into materials involving strongly correlated electrons that are challenging for the traditional condensed matter paradigm (see, e.g., [8; 9]).

The Lifshitz spacetime is one of the famous example as a possible dual to nonrelativistic systems. This spacetime has a scale invariance

$$t \to \lambda^z t, \quad x \to \lambda x, \quad z \neq 1 \tag{1.1}$$

called "dynamic scaling", which is found in fixed points governing phase transitions in many condensed matter systems. It has been shown that the boundary to bulk mapping via

smearing functions breaks down for the pure Lifshitz spacetime [11]. Moreover, in bosonic AdS/CFT, the boundary Green's function, which is expected to probe the entire bulk from the boundary to the horizon, becomes exponentially insensitive in the low-energy limit [12].

The main goal of this thesis is to investigate the boundary Green's function from the Lifshitz background using fermionic AdS/CFT.[1] Since the fermions couple to gravity differently from bosons, it is reasonable to ask whether the insensitivity of Green's function is also observed in the fermionic theory.

The result of our analysis is that the pattern holds for the Lifshitz $z = 2, 3, 4$ backgrounds in the fermionic theory. This thesis is organized as follows. In section 2, we review the bosonic AdS/CFT in the AdS and Lifshitz backgrounds, and explain the major techniques, namely, the analytic method, the WKB approximation, and the numerical method. In section 3, we apply the same techniques to calculate the boundary Green's function and the spectral function using fermionic AdS/CFT from the AdS and Lifshitz backgounds, and discuss some of its feature similar to the bosonic cases.

[1] In this thesis, we follow the AdS/CFT prescription with spinors formulated in [17].

Chapter 2

Review of Non-relativistic AdS/CFT with Bosons

2.1 Calculating the Green's function via AdS/CFT

In this section, we outline the holographic calculation of the field theory Green's function. The scalar Green's function is obtained from the boundary of bulk spacetime, in which we calculate the equation of motion of a scalar particle coupled to gravity. The scalar field equation in a curved space is obtained from the action:

$$\mathcal{S} = \int \sqrt{-g}[-g^{\mu\nu}\partial_\mu\phi\partial_\nu\phi - m^2\phi^2]d^n x \tag{2.1}$$

By the variational principle, the field equation is obtained as

$$\frac{1}{\sqrt{-g}}\partial_\mu(\sqrt{-g}g^{\mu\nu}\partial_\nu\phi) - m^2\phi = 0 \tag{2.2}$$

For the pure AdS_{n+2} and Lifshitz geometry we are considering, the metric is given by [1]

$$ds^2 = -\left(\frac{L}{r}\right)^{2z} dt^2 + \left(\frac{L}{r}\right)^2 (d\vec{x}_n^2 + dr^2). \tag{2.4}$$

Then the field equation (2.2) takes the form of

$$-r^{2z}\partial_t^2\phi + r^2\partial_i^2\phi + (-z-n+1)r\partial_r\phi + r^2\partial_r^2\phi - m^2\phi = 0 \tag{2.5}$$

where i runs over the spatial indices and we set $L = 1$. Since we are mainly interested in the Green's function in terms of energy ω and momentum $\vec{k}$, we move to momentum space.

$$\phi(r) = e^{i(\vec{k}\cdot\vec{x}-\omega t)} f(r) \tag{2.6}$$

Then we obtain the following equation for the radial wavefunction.

$$r^2 f''(r) + (-z-n+1)rf'(r) + (r^{2z}\omega^2 - r^2k^2 - m^2)f(r) = 0 \tag{2.7}$$

where $k = |\vec{k}|$.

According to the holographic prescription to calculate the boundary retarded Green's function, we need to impose infalling boundary conditions to the radial wavefunction. For our coordinate system, we have $r \to 0$ as the boundary, and $r \to \infty$ as the horizon. The infalling particle means that it only approaches to the horizon, but does not escape from it. To set up this boundary condition, we need to examine the asymptotic form of the wavefunction at $r \to \infty$. The condition is slightly different for the AdS background $z = 1$ and the Liftshitz background $z > 1$. For the AdS case, by taking the limit $r \to \infty$, one can find the radial wavefunction $f(r)$ assumes

$$f(r) = r^{n/2}(ae^{iqr} + be^{-iqr}), \quad q = \sqrt{\omega^2 - k^2}, \tag{2.8}$$

[1] This geometry was well studied in [12]. In that paper, the following form of metric was used.

$$ds^2 = \left(\frac{L}{z\rho}\right)^2 (-dt^2 + d\rho^2) + \left(\frac{L}{z\rho}\right)^{2/z} d\vec{x}_n^2 \tag{2.3}$$

This transforms to ours with scaling $\rho \to (L/z)r^z, t \to Lt$, and $\vec{x} \to L\vec{x}$.

where a and b are some constants. If we restrict ourselves to $q > 0$, the first term is the infalling wave, and the second term is the outgoing wave. Then the infalling boundary condition means $b = 0$.

For the Lifshitz case, it is easier if we transform the radial equation (2.7) to the Schrödinger like equation. By scaling $f(r) \to r^{(z+n-1)/2} f(r)$, one gets

$$-f''(r) + Uf(r) = 0, \quad U = \frac{\nu^2 - 1/4}{r^2} - r^{2(z-1)}\omega^2 + k^2, \tag{2.9}$$

with the effective potential U and the effective energy 0. In the limit $r \to \infty$, the potential U approaches to $U \sim -r^{2(z-1)}\omega^2$. We try the WKB approximation in the classical region, which results in

$$f(r) = \frac{C}{\sqrt[4]{-U}} \exp[\pm i \int \sqrt{-U} dr] = C \frac{r^{n/2}}{\sqrt{\omega}} \exp[\pm i\omega r^z/z]. \tag{2.10}$$

By reversing the scaling $r^{(z+n-1)/2} f(r) \to f(r)$, we get the following limiting form near horizon.

$$f(r \to \infty) = r^{n/2}(ae^{i\omega r^z/z} + be^{-i\omega r^z/z}) \tag{2.11}$$

Again, the infalling boundary condition means that we drop the outgoing wave, $b = 0$.

With the boundary condition and the differential equation (2.7), one can completely determine the radial wavefunction $f(r)$. The next step of the holographic calculation is to inspect the boundary behavior of $f(r)$. The asymptotic form of $f(r)$ near boundary can be obtained from the radial equation (2.7) by taking the limit $r \to 0$ and trying the power series solution $f(r) = r^\alpha$, which results in

$$f(r \to 0) = Ar^{\frac{z+n}{2} - \nu} + Br^{\frac{z+n}{2} + \nu}, \quad \nu = \sqrt{m^2 + \left(\frac{z+n}{2}\right)^2}. \tag{2.12}$$

When r approaches 0, the second term converges to 0, but the first term diverges to the infinity. According to AdS/CFT, the boundary Green's function is equal to the ratio of the

normalizable mode B to the non-normalizable mode A, i.e.,

$$G(\omega, \vec{k}) = K\frac{B}{A} \tag{2.13}$$

for some normalization constant K. In addition, the spectral function is captured in the imaginary part of the Green's function by

$$\chi(\omega, \vec{k}) = 2ImG_R(\omega, \vec{k}), \tag{2.14}$$

which gives the density of states in the boundary theory.

In case when the differential equation (2.7) can be solved exactly and we can obtain the radial wavefuction $f(r)$ in a closed form, we can also obtain the retarded Green's function exactly through AdS/CFT. If we cannot get the exact $f(r)$, then we can try to solve it numerically. In either case, we will be able to see how the Green's function probes the pure AdS and Lifshitz geometry, and how it is different for the relativistic and non-relativistic spacetimes.

Lastly, we remark that the Green's function is expected to possess the scale-invariance inherited from the bulk geometry. That is to say, the AdS and Lifshitz metric is scale-invariant under the scaling,

$$t \to \lambda^z t, \quad , \vec{x} \to \lambda\vec{x}, \quad r \to \lambda r, \tag{2.15}$$

from which the momentum is scaled by,

$$\vec{k} \to \frac{\vec{k}}{\lambda}, \quad \omega \to \frac{\omega}{\lambda^z}, \tag{2.16}$$

which is deduced from the plane wave solution (2.6). Let us consider that the Green's function is spherically symmetric. If the Green's function is scale-invariant, it only picks up a constant under scaling by

$$G(\omega, k) \to \lambda^s G(\omega, k) \tag{2.17}$$

for some constant s. By expanding the Green's function into a power series in ω and k and choosing only the terms with appropriate scaling behavior, we find that the Green's function behaves as

$$G(\omega, k) = ak^s + b\omega^{s/z} + c\omega s/z\zeta(\frac{k}{\omega^{1/z}}) \tag{2.18}$$

for some constant a, b, and c and some function ζ. Therefore we expect that the Green's function we calculate to be consistent with the above expression.

2.2 The Exact Green's function for the AdS_{n+2} and Lifshitz $z = 2$ Backgrounds

In this section, we calculate the retarded Green's function in the closed forms for the AdS_{n+2} and the Lifshitz $z = 2$ backgrounds, using the AdS/CFT prescription. Then we discuss some features of the spectral functions, especially those unique in the non-relativistic case ($z = 2$).

In the AdS_{n+2} background ($z = 1$), the solution to the differential equation (2.7) is a linear combination of Bessel functions.

$$f(r) = r^{(n+1)/2}(C_1 J_\nu(qr) + C_2 Y_\nu(qr)), \quad q = \sqrt{\omega^2 - k^2} \tag{2.19}$$

If we restrict ourselves to $\nu > 0$, the asymptotic forms near horizon of Bessel functions are given by

$$J_\nu(qr \to \infty) \sim \sqrt{\frac{2}{\pi qr}} cos(qr - \frac{\pi\nu}{2} - \frac{\pi}{4}) \tag{2.20}$$

$$Y_\nu(qr \to \infty) \sim \sqrt{\frac{2}{\pi qr}} sin(qr - \frac{\pi\nu}{2} - \frac{\pi}{4}). \tag{2.21}$$

Using these forms, one can find the coefficients C_1 and C_2 that match to the infalling boundary condition $f(r \to \infty) = ae^{iqr}$. Then we expand $f(r)$ near the boundary, using the

asymptotic forms of Bessel functions.

$$J_\nu(qr \to 0) \sim \frac{1}{\Gamma(\nu+1)}\left(\frac{qr}{2}\right)^\nu \tag{2.22}$$

$$Y_\nu(qr \to 0) \sim -\frac{1}{\pi}\left[cos(\pi\nu)\Gamma(-\nu)\left(\frac{z}{2}\right)^\nu - \Gamma(\nu)\left(\frac{qr}{2}\right)^{-\nu}\right] \tag{2.23}$$

Then we identify the coefficient of $r^{(n+1)/2-\nu}$ as A and $r^{(n+1)/2+\nu}$ as B, which gives the following response to source ratio, which is the retarded Green's function of boundary theory.

$$G_R(q) = K\frac{B}{A} = Ke^{-i\pi\nu}\frac{\Gamma(-\nu)}{\Gamma(\nu)}\left(\frac{q}{2}\right)^{2\nu} \tag{2.24}$$

We observe that the Green's function and the spectral function from the AdS background is proportional to $(\omega^2 - k^2)^\nu$, which obeys the expected behavior argued from the scale-invariance.

For the Lifshitz background $z = 2$, the solution to the differential equation is found to be a linear combination of the Kummer's confluent hypergeometric functions $U(a, b, z)$ and $M(a, b, z)$ by

$$f(r) = e^{-ir^2\omega/2}r^{(n+2)/2+\nu}[C_1U(a, b, ir^2\omega) + C_2M(a, b, ir^2\omega)] \tag{2.25}$$

where a and b are given by

$$a = \frac{1}{2}(-i\alpha + \nu + 1), \quad b = \nu + 1, \quad \alpha = \frac{k^2}{2\omega}. \tag{2.26}$$

Again, we match the limiting form of $f(r)$ at $r \to \infty$ to the infalling boundary condition $f(r \to \infty) = ar^{n/2}e^{i\omega r^2/2}$. At a large variable, U and M become

$$U(a, b, |z| \to \infty) \sim (z)^{-a} \tag{2.27}$$

$$M(a, b, |z| \to \infty) \sim \frac{\Gamma(b)}{\Gamma(a)}e^z z^{a-b} + \frac{\Gamma(b)}{\Gamma(b-a)}(-z)^{-a}. \tag{2.28}$$

Using these expressions, one can find C_1 and C_2 in terms of a. For our calculation, we only need the ratio C_2/C_1, which is

$$\frac{C_2}{C_1} = -e^{-i\pi a}\frac{\Gamma(b-a)}{\Gamma(b)} \tag{2.29}$$

To find the source A and the response B, we expand $f(r)$ near boundary using the limiting forms of U and M at a small variable given by

$$U(a, b, |z| \to 0) = z^{-b+1}\frac{\Gamma(b-1)}{\Gamma(a)} + \frac{\Gamma(1-b)}{\Gamma(1+a-b)} \tag{2.30}$$

$$M(a, b, |z| \to 0) = 1. \tag{2.31}$$

Then one obtains the expression for A and B in terms of C_1 and C_2. From its ratio, the retarded Green's function is found as

$$G_R = K\frac{B}{A} = \omega^\nu e^{-i\pi\nu/2}\frac{\Gamma(-\nu)\Gamma((i\alpha+\nu+1)/2)}{\Gamma(\nu)\Gamma((i\alpha-\nu+1)/2)}, \quad \alpha = \frac{k^2}{2\omega} \tag{2.32}$$

Similar to the AdS case, we find that the Green's function shows the power law behavior, ω^ν. The spectral function constructed from it shares the general features with that of the AdS case, i.e., the growth with increasing ω and the decline with increasing k (see figure 2.1). What's interesting is the factor α in the gamma function. For the large ω limit, or equivalently $\alpha \ll \nu$, the role of α in the gamma funtion is not significant, and the behavior is dominated by the monomial factor ω^ν. However, for the small ω, namely $\alpha \gg \nu$, the α factor becomes significant. Using the Euler's reflection formula $\Gamma(1-z)\Gamma(z) = \pi/sin(\pi z)$ and the Stirling's approximation $\Gamma(z) \sim \exp[(z-1/2)\log z - z]\sqrt{2\pi}(1+O(z^{-1}))$ for the large variable, one finds the leading term as

$$G_R(\omega, \vec{k}) \sim K\frac{\Gamma(-\nu)}{\Gamma(\nu)}\left(\frac{k}{2}\right)^{2\nu}(1 + e^{-i\pi\nu}e^{-\pi\alpha}), \quad \alpha \gg \nu, \tag{2.33}$$

and the spectral function can be found immediately as

$$\chi(\omega, \vec{k}) = -2K\frac{\Gamma(-\nu)}{\Gamma(\nu)}\left(\frac{k}{2}\right)^{2\nu}\sin(\pi\nu)e^{-\pi\alpha}, \quad \alpha \gg \nu. \tag{2.34}$$

This result shows that in the large α limit, the spectral function vanishes by the exponential factor $e^{-\pi\alpha}$. That is, in the region of momentum space $k^2/\nu \gg \omega$, χ is suppressed exponentially. This is a pattern not found in the AdS spacetime (see figure 2.2 and 2.3). With more careful analysis done in [12], it can also be shown that the Green's function is insensitive to the change of horizon boundary condition in this limit. For example, changing the boundary condition from the infalling one to the outgoing one will have an exponentially small influence on the Green's function. Moreover, according to the Minkowski AdS/CFT, the infalling boundary condition gives the retarded Green's function, and the outgoing boundary condition gives the advanced Green's function. In this case, the spectral function is given by

$$\chi(\omega, \vec{k}) = 2ImG_R(\omega, \vec{k}) = -i(G_R(\omega, \vec{k}) - G_A(\omega, \vec{k})). \tag{2.35}$$

Since the spectral function becomes exponentially small in this limit, the effect of changing boundary condition also gets harder to be seen through it. This implies that the low-energy physics is hidden from the boundary, and the transition to such low-energy physics occurs at $k^2/\omega \sim \nu$ in the Lifshitz $z = 2$ background. This pattern is also observed for the $z > 2$ cases, which is the subject of next section.

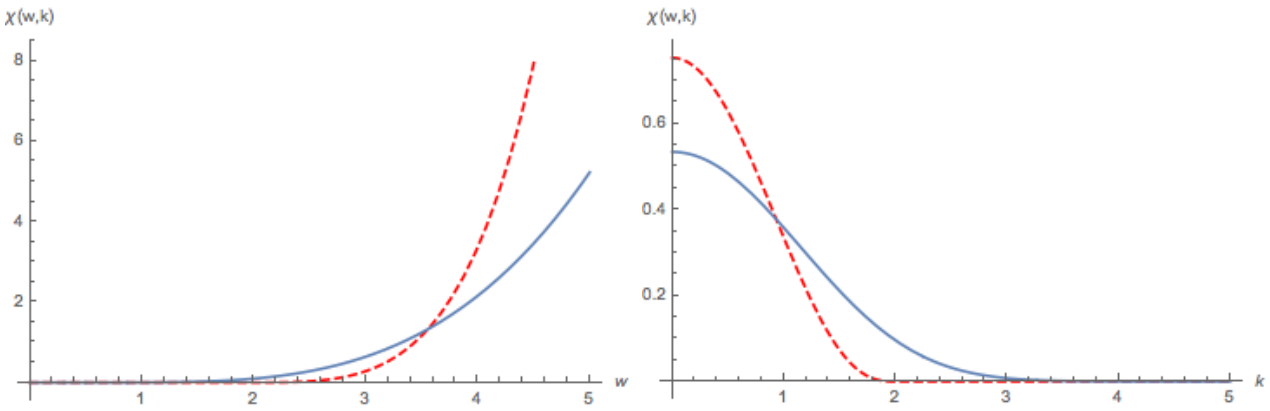

Figure 2.1 The exact spectral functions for the AdS background (dashed) and the Lifshitz background (continous) with fixed $k = 2$ (left plot) and with fixed $w = 2$ (right plot) for $m = 2$.

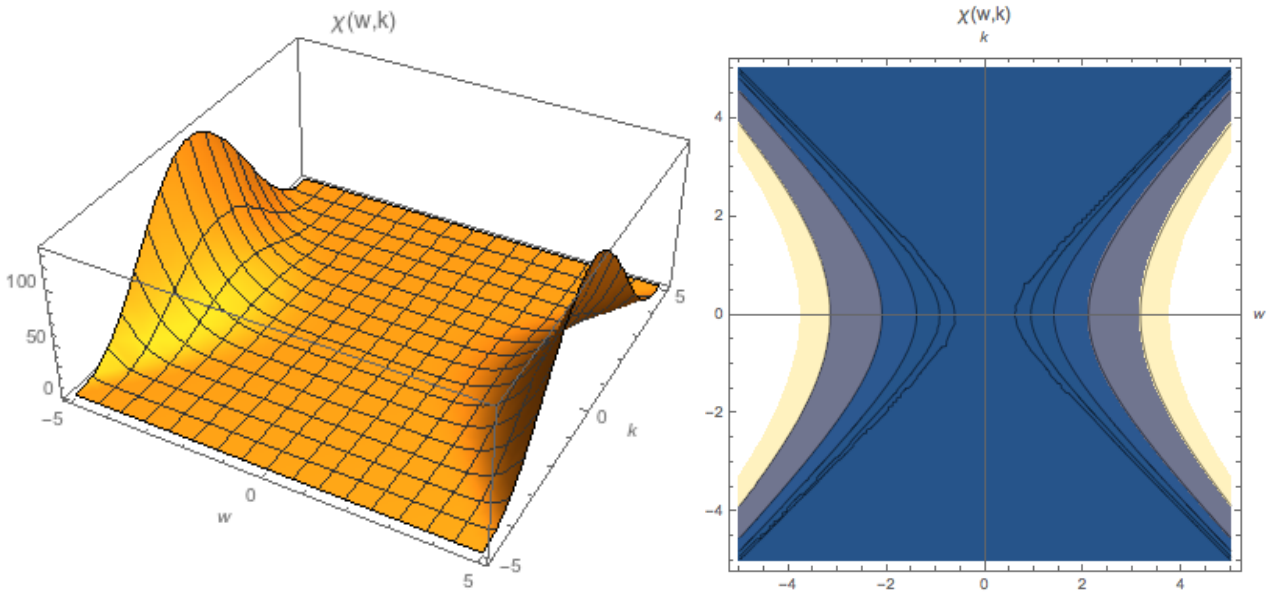

Figure 2.2 The exact spectral function for the AdS background with $m = 2$. The contour lines were drawn at $|\chi(\omega, k)| = 10, 1, 0.1, 0.01, 0.001$. The contours converge to $k = \omega$ line, manifesting the relativistic energy relation $\omega^2 = k^2 + m^2$.

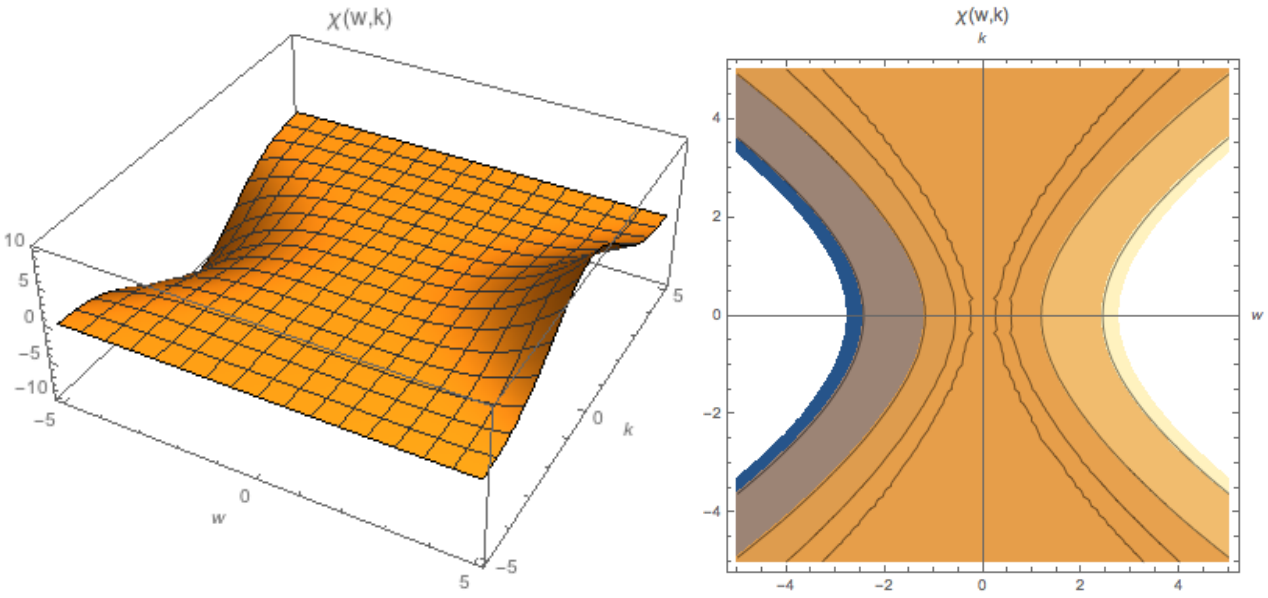

Figure 2.3 The exact spectral function for the Lifshitz $z = 2$ background with $m = 2$. The contour lines were drawn at $|\chi(\omega, k)| = 10, 1, 0.1, 0.01, 0.001$. Compared to the relativistic case, we see that the contours are sparsely distributed in the region of small ω. Moreover, the contours are similar to the curve $k^2/\omega \sim \nu$, rather than $k = \omega$.

2.3 WKB Approximation for the Lifshitz $z > 1$ Backgrounds

In this section, we analyze the process that the horizon information reaches the boundary from the viewpoint of tunneling barrier and WKB approximation. This approach will generalize the feature of spectral functions at the low-energy found from the analytic method for the $z = 2$ case to the $z > 2$ cases. The starting point is the Schrödinger like form of the radial differential equation (2.9) we obtained earlier by scaling $f(r) \to r^{(z+n-1)/2} f(r)$.

$$-f''(r) + Uf(r) = 0, \quad U = \frac{\nu^2 - 1/4}{r^2} - r^{2(z-1)}\omega^2 + k^2, \tag{2.36}$$

We think of this equation as representing a particle with an effective energy 0 in an effective potential U. While the WKB approximation is only valid when the potential is varying slowly, the analysis in [11] showed that it is applicable to our potential if we make a shift $\nu^2 \to \nu^2 + 1/4$. The classical turning point r_0 is given by $U(r_0) = 0$, and the WKB approximation gives the following wavefunctions in the tunneling and classical regions.

$$f_{\mathrm{WKB}}(r < r_0) = \frac{1}{\sqrt[4]{U}}(Ce^{\int_r^{r_0} dr\sqrt{U}} + De^{\int_r^{r_0} dr\sqrt{U}}) \tag{2.37}$$

$$f_{\mathrm{WKB}}(r > r_0) = \frac{1}{\sqrt[4]{-U}}(ae^{i\int_r^{r_0} dr\sqrt{-U}} + be^{-i\int_r^{r_0} dr\sqrt{-U}}) \tag{2.38}$$

The connection between two region is obtained by approximating the potential near the turning point by a linear potential, i.e., $U \sim -U_0(r - r_0)$. The solution of Schrödinger equation for this potential is known as the Airy functions, and matching their asymptotic forms with f_{WKB} in both regions gives the connection formula.

$$\begin{pmatrix} C \\ D \end{pmatrix} = \begin{pmatrix} e^{-i\pi/4} & e^{i\pi/4} \\ \frac{1}{2}e^{i\pi/4} & \frac{1}{2}e^{-i\pi/4} \end{pmatrix} \begin{pmatrix} a \\ b \end{pmatrix} \tag{2.39}$$

The next step is to join $f_{\rm WKB}$ with the boundary form of the exact wavefunction in order to find the source and response. The boundary limit of $f(r)$ is found from the Schrödinger equation (2.36) as

$$f_{exact}(r \to 0) = Ar^{\frac{1}{2}-\nu} + Br^{\frac{1}{2}+\nu}. \tag{2.40}$$

We want the $f_{\rm exact}$ and $f_{\rm WKB}$ to be joined up to its first derivative at some point $r = \epsilon$, which we send to 0 at the end. The connection is expressed in a compact form, first by defining

$$f_{\rm exact}(r \to 0) = Af_1 + Bf_2$$
$$f_{\rm WKB}(r < r_0) = Cf_3 + Df_4.$$

Then the two expression is tied by

$$\begin{pmatrix} A \\ B \end{pmatrix} = \frac{1}{W_{12}} \begin{pmatrix} W_{32} & W_{42} \\ W_{13} & W_{14} \end{pmatrix} \begin{pmatrix} C \\ D \end{pmatrix}, \quad W_{ij} \equiv (f_i f_j' - f_i' f_j)|_{r=\epsilon} \tag{2.41}$$

where W_{ij} are found to be

$$W_{12} = 2\nu, \quad W_{32} = 2\sqrt{\nu}\epsilon^{\nu} e^{\int_{\epsilon}^{r_0} dr\sqrt{U}}, \quad W_{14} = 2\sqrt{\nu}\epsilon^{-\nu} e^{-\int_{\epsilon}^{\epsilon_0} dr\sqrt{U}}, \quad W_{13} = W_{42} = 0.$$

Now we can find the Green's function and the spectral function from the response to source ratio B/A. For the infalling boundary condition $b = 0$, the spectral function is found as

$$\chi(\omega, \vec{k}) = 2ImG(\omega, \vec{k}) = \frac{K}{\sqrt{\nu}} \epsilon^{-2\nu} \exp[-2\int_{\epsilon}^{r_0} dr\sqrt{U}]. \tag{2.42}$$

From this expression, we find that the exponential suppression comes from the form of potential U. We can obtain more precise behavior of the spectral function by working out the integral. For example, let us consider the potential U for the $z = 2$ case in the large k^2/ω limit. The potential is given by

$$U = \frac{\nu^2}{r^2} - r^2\omega^2 + k^2. \tag{2.43}$$

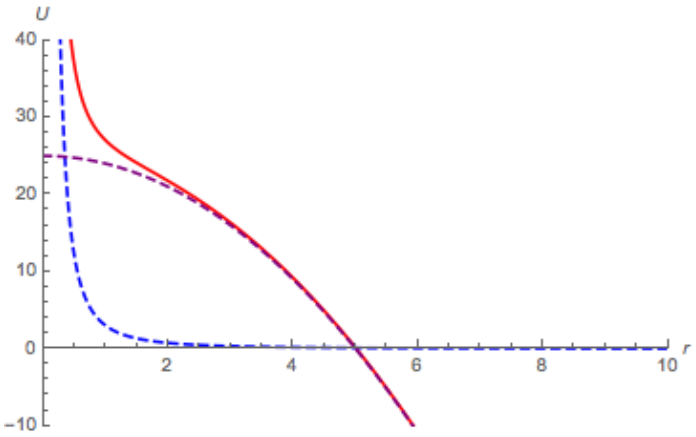

Figure 2.4 The potential $U = \nu^2/r^2 - r^2\omega^2 + k^2$ for $\nu = 3$, $\omega = 1$, and $k = 5$ (red line). The blue dashed line and the purple dashed line represent ν^2/r^2 and $-r^2\omega^2 + k^2$. The potential is close to the first term before $r_* \sim \nu/k$, and close to the last two terms beyond this point.

When $r < r_* \sim \nu/k$, the first term ν^2/r^2 dominates. Beyond r_*, this term falls off quickly, and the potential can be approximated by the last two terms up to the classical turning point r_0 (see figure 2.4). Therefore we divide the scope of integration into two regions by

$$\int_\epsilon^{r_*} \sqrt{\frac{\nu^2}{r^2}} dr + \int_{r_*}^{r_0} \sqrt{-r^2\omega^2 + k^2} dr \tag{2.44}$$

The first integration provides $\sim (\epsilon\omega)^{2\nu}$ in the spectral function, which cancels $\epsilon^{-2\nu}$ and gives a power law behavior. It is the second integration that introduces the suppression factor $\exp[-\frac{\pi}{4}\frac{k^2}{\omega}]$ into the spectral function, which is equal to the exponential factor that we found from the analytic method. Therefore we observe that in the view of the Shrödinger equation, the potential that falls off slower than $\sim 1/r^2$ and extends to the classical turning point gives rise to the exponential decay of the wavefunction near boundary.

Finally, we remark that, while we discussed for the $z = 2$ case here, the same pattern holds for the higher values of z in the Lifshitz background. The asymptotic behavior of the spectral function $\chi_{\text{WKB}} \sim \exp[-\lambda\alpha^{1/\zeta}]$ for the general values of z was worked out in [12],

where the constants are given by

$$\lambda = \frac{\sqrt{\pi}\Gamma(1/\zeta - 1/2)}{2\Gamma(1/\zeta)}, \quad \alpha = \left(\frac{\omega}{z}\right)^{\zeta}\left(\frac{k}{\omega}\right)^{2}, \quad \zeta = 2(1-\frac{1}{z}). \tag{2.45}$$

Our main goal of this thesis is to see whether the exponential decoupling of horizon is observed in AdS/CFT with spinors. If so, our next question will be whether the above formula also carries over, which will be addressed in the second chapter.

2.4 Numerical Approximation

As another way of investigating the Lifshitz background for higher z, we discuss the numerical approximation. This also serves as a consistency check of the earlier derivations with the exact method and the WKB approximation. The general scheme to obtain the boundary Green's function is the same as that used for the analytic calculation. The only difference is that we solve the radial differential equation (2.7) numerically. With the infalling boundary condition, one can integrate the differential equation from sufficiently large r to $r \sim 0$. Then we fit the numerical solution to the asymptotic form near boundary to find the source A and the response B. The asymptotic form near boundary is given by,

$$f(r) = Ar^{\frac{z+n}{2}-\nu}(1+\alpha_1 r+\alpha_2 r^2+...) + Br^{\frac{z+n}{2}+\nu}(1+\beta_1 r+\beta_2 r^2+...). \tag{2.46}$$

We can improve the precision by including higher order terms, but fitting does not give a good result for B, as it is overwhelmed by A. Therefore we first obtain A, and strip off the phase of A, $phA = e^{i\phi}$ ($\phi = argA$) from the numerical solution for $f(r)$. Then we take the imaginary part of this stripped solution, to obtain the imaginary part of response divided by the phase of A, i.e., $Im[e^{-\phi}B]$.

$$Im[e^{-i\phi}f(r)] = Im[e^{-i\phi}B]r^{\frac{z+d}{2}+\nu}(1+\beta_1 r+\beta_2 r^2+...) \tag{2.47}$$

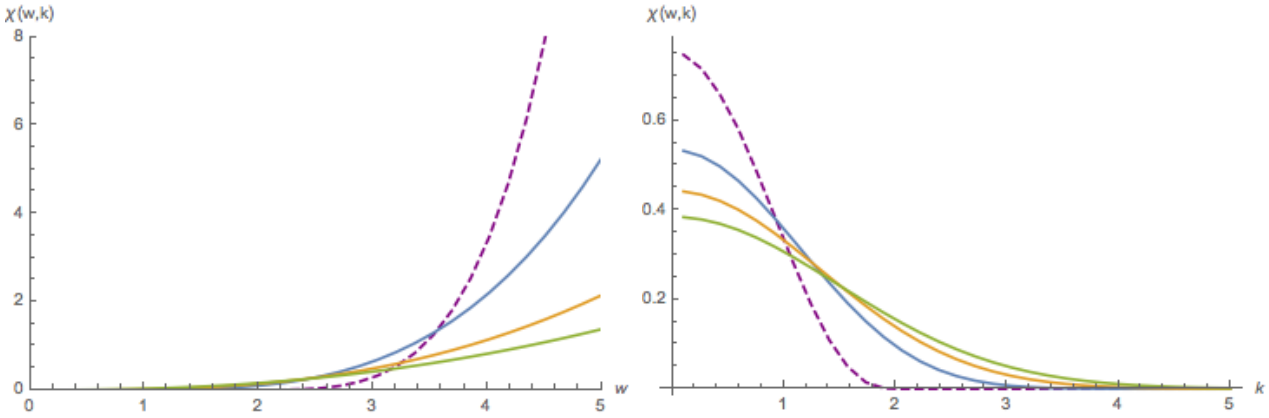

Figure 2.5 The holographic spectral function calculated numerically from the AdS (dashed) and the Lifshitz $z = 2, 3, 4$ (blue, orange, green) backgrounds for $k = 2$, $m = 2$ (left plot) and for $w = 2$, $m = 2$ (right plot).

This gives the enough information to construct the imaginary part of the Green's function, from which we can obtain the spectral function.

$$Im[G(w, \vec{k})] = KIm[\frac{B}{A}] = K\frac{Im[e^{-i\phi}B]}{|A|} \tag{2.48}$$

The numerical calculation of spectral functions is consistent with the previous analysis with a few percent error for the AdS and Lifshitz $z = 2$ cases. In general, the spectral functions from the pure AdS and pure Lifshitz spacetime shows the power law behavior (see figure 2.5), which is consistent with the scale invariance of theory. Overall, the numerical calculation is proven useful, and we will revisit this approach in the analysis of fermionic AdS/CFT.

Chapter 3

Non-relativistic AdS/CFT with Fermions

3.1 Spinors in the Curved Spacetime

In this section, we summarize the derivation of the field equation for the radial coordinate r. As for the bosonic case, we start from the field equation in a flat spactime. The fermions are described by the Dirac equation,[1]

$$(\gamma^{\bar{\mu}}\partial_\mu - m)\psi = 0 \tag{3.1}$$

where the gamma matrix satisfies $\{\gamma^{\bar{\mu}}, \gamma^{\bar{\nu}}\} = \eta^{\bar{\mu}\bar{\nu}}$. In a curved spacetime, a different treatment is required for the gamma matrix and the derivative of spinor fields ψ. That is, the anticommutation relation becomes

$$\{\gamma^\mu, \gamma^\nu\} = 2g^{\mu\nu} \tag{3.2}$$

and we replace the partial derivative with the local Lorentz covariant derivative, namely,

$$\nabla_\mu\psi = \partial_\mu\psi + \frac{1}{4}\omega_{\mu\nu\lambda}\gamma^{\nu\lambda}\psi \tag{3.3}$$

[1]Used the bar to indicate the flat spacetime only in this section.

where $\gamma^{\mu\nu}$ is defined as $\frac{1}{2}[\gamma^\mu, \gamma^\nu]$ and $\omega_{\mu\nu\lambda}$ is known as the spin connection.[2] For the diagonal metric we consider, it can be obtained as

$$\omega_{\mu\nu\lambda} = g_{\mu[\nu,\lambda]} = \frac{1}{2}(g_{\mu\nu,\lambda} - g_{\mu\lambda,\nu}). \tag{3.4}$$

Let us consider a general form of a diagonal metric,

$$ds^2 = -e^{2A(r)}dt^2 + e^{2B(r)}d\vec{x}_n^2 + e^{2C(r)}dr^2 \tag{3.5}$$

where n denotes the number of spatial dimensions. Then one finds the four non-vanishing spin connections, which are

$$\omega_{ttr} = -\omega_{trt} = -\frac{dA}{dr}e^{2A}, \quad \omega_{iir} = -\omega_{iri} = \frac{dB}{dr}e^{2B} \tag{3.6}$$

With these expressions, the Dirac equation assumes the following form.[3]

$$(\not{\nabla} - m)\psi = (\gamma^t\partial_t + \gamma^i\partial_i + \gamma^r\partial_r + \frac{1}{2}\gamma^r(A' + nB') - m)\psi = 0 \tag{3.7}$$

Further simplification is possible through scaling, $\psi \to e^{-\frac{1}{2}(A+nB)}\psi$, which eliminates the $\frac{1}{2}\gamma^r(A'+nB')$ term. In addition, we can express the gamma matrices in the curved spacetime in terms of those in the flat spacetime. Noticing the relations, $\gamma^{\bar{\mu}}\gamma^{\bar{\mu}} = \eta^{\bar{\mu}\bar{\mu}}$ and $\gamma^\mu\gamma^\mu = g^{\mu\mu}$, one finds

$$\gamma^t = \gamma^{\bar{t}}e^{-A}, \quad \gamma^t = \gamma^{\bar{i}}e^{-B}, \quad \gamma^t = \gamma^{\bar{r}}e^{-C}. \tag{3.8}$$

We can proceed further by working in the momentum space. We consider a plane wave solution, $\psi = e^{i(\vec{k}\cdot\vec{x}-\omega t)}f(r)$. By putting together, one finds the following equation for the radial coordinate.

$$(e^{-A}\gamma^{\bar{t}}(-it) + e^{-B}\gamma^{\bar{i}}(ik_i) + e^{-C}\gamma^{\bar{r}}\partial_r - m)f(r) = 0 \tag{3.9}$$

[2]For the more detailed formulation in terms of the frame field for fermions coupled to gravity, see [18].

[3]The tensor operation is still done using the Minkowski metric.

Our next task is to find the solution for $f(r)$, and use the AdS/CFT prescription to obtain the boundary Green's function, as outlined in [17]. The exact solution is possible for the pure AdS background. However, we resort to the numerical method for the Lifshitz background.[4]

3.2 The Exact Green's function for the AdS$_{n+2}$ Background

In this section, we obtain the exact radial wavefunction $f(r)$ the pure AdS$_{n+2}$ background, calculate the boundary Green's function, and examine the spectral function. While the retarded Green's function for this background was worked out before in [17], we use a different coordinate system for r and use the Weyl basis. The result will also serve as a check for our numerical calculation later. The AdS$_{n+2}$ metric is given by

$$ds^2 = \left(\frac{L}{r}\right)^2 (-dt^2 + d\vec{x}_n^2 + dr^2). \tag{3.10}$$

We choose the Weyl basis for the representation of gamma matrix, as the Dirac equation takes a simpler form than that with the Dirac basis.

$$\gamma^t = i\begin{pmatrix} 0 & 1 \\ 1 & 0 \end{pmatrix}, \quad \gamma^i = i\begin{pmatrix} 0 & \sigma^i \\ \sigma^i & 0 \end{pmatrix}, \quad \gamma^r = \begin{pmatrix} -1 & 0 \\ 0 & 1 \end{pmatrix} \tag{3.11}$$

Using this representation, one finds the Dirac equation (3.9) takes the form of

$$\begin{pmatrix} -\partial_r - m/r & \omega - \vec{k}\cdot\vec{\sigma} \\ \omega + \vec{k}\cdot\vec{\sigma} & \partial_r - m/r \end{pmatrix} f(r) = 0, \quad f(r) = \begin{pmatrix} f_a(r) \\ f_b(r) \end{pmatrix} \tag{3.12}$$

where we set $L = 1$ for convenience and divided $f(r)$ into the upper and lower parts. This equation can be decoupled into two second order linear differential equations for f_a and f_b,

[4]For m = 0, the exact solution was worked out in [16].

which are

$$[\partial_r^2 + \omega^2 - k^2 - \frac{1}{r^2}(\nu_\pm^2 - \frac{1}{4})]f_{a/b}(r) = 0, \quad \nu_\pm = m \pm \frac{1}{2}. \tag{3.13}$$

This equation has the Bessel functions as solutions. One can find a complete set of solutions by first expressing f_a in terms of the Bessel functions, and by plugging it into (3.12) to find f_b. That is to say, the solutions for f_a and f_b are

$$f_a(r) = \sqrt{r}(C_1 J_{\nu+}(qr) + C_2 Y_{\nu+}(qr)), \tag{3.14}$$

$$f_b(r) = \left(\frac{\omega + \vec{k}\cdot\vec{\sigma}}{q}\right)\sqrt{r}(C_1 J_{\nu-}(qr) + C_2 Y_{\nu-}(qr)) \tag{3.15}$$

where $q = \sqrt{\omega^2 - k^2}$ and we also used the identity $J'_\nu(z) = J_{\nu-1}(z) - \frac{\nu}{z}J_\nu(z)$ to obtain the second expression.

Now we follow the AdS/CFT prescription with spinnors to obtain the retarded Green's function. We first impose the infalling boundary condition as follows.

$$f_a(r \to \infty) = ae^{iqr}, \quad f_b(r \to \infty) = \frac{\omega + \vec{k}\cdot\vec{\sigma}}{q} iae^{iqr} \tag{3.16}$$

Here a is a constant vector, and we restrict the momentum to be timelike $w > |\vec{k}|$ so that q is real. To match the boundary condition and our solution, it is convenient to use the Hankel functions, which are related to the Bessel functions as

$$H_\nu^{(1)}(z) = J_\nu(z) + iY_\nu(z), \quad H_\nu^{(2)}(z) = J_\nu(z) - iY_\nu(z) \tag{3.17}$$

and whose asymptotic forms are

$$H_\nu^{(1)}(|z| \to \infty) \sim \sqrt{\frac{2}{\pi z}}e^{i(z - \frac{1}{2}\nu\pi - \frac{1}{4}\pi)}, \quad H_\nu^{(2)}(|z| \to \infty) \sim \sqrt{\frac{2}{\pi z}}e^{-i(z - \frac{1}{2}\nu\pi - \frac{1}{4}\pi)}. \tag{3.18}$$

By comparing these forms with the infalling boundary condition, one finds that the radial wavefunctions assume

$$f_a(r) = \sqrt{\frac{\pi qr}{2}}e^{i(\nu_+\pi/2 + \pi/4)} a H_{\nu_+}^{(1)}(qr) \tag{3.19}$$

$$f_b(r) = \frac{\omega + \vec{k}\cdot\vec{\sigma}}{q}\sqrt{\frac{\pi q r}{2}}e^{-i(\nu_+ \pi/2+\pi/4)}iaH^{(1)}_{\nu_-}(qr). \tag{3.20}$$

Meanwhile, one can show from the Dirac equation (3.12) that the limiting form of the wavefunctions near the boundary are

$$f_a(r\to 0) = Ar^{-m} + Br^{m+1}, \quad f_b(r\to 0) = Cr^{-m+1} + Dr^m. \tag{3.21}$$

where the coefficients are related as $(2m+1)B = (\omega - \vec{k}\cdot\vec{\sigma})D$ and $(2m-1)C = (\omega+\vec{k}\cdot\vec{\sigma})A$. We identify the term Ar^{-m} as the non-normalizable mode, and the term Dr^m as the normalizable mode. Let them be related by $D = \mathcal{S}A$. According to the AdS/CFT recipe, A corresponds to the source, D corresponds to the expectation value, and the retarded Green's function is given as

$$G_R = -i\mathcal{S}\gamma^t \tag{3.22}$$

where $\gamma^0 = i\sigma^t = i$ in our basis.

Now we examine the limiting form of equations (3.20) at the boundary to find the coefficients A and B. We restrict ourselves to the case $\nu_\pm > 0$. Then the Hankel function in (3.20) takes the limiting form of

$$\begin{aligned} H^{(1)}_{\nu_\pm}(|z|\to 0) &= J_{\nu_\pm}(z) + iY_{\nu_\pm}(z) \\ &= \frac{(z/2)^{\nu_\pm}}{\Gamma(\nu_\pm+1)} - \frac{i}{\pi}\left[\Gamma(\nu_\pm)\left(\frac{z}{2}\right)^{-\nu_\pm} + cos(\pi\nu)\Gamma(-\nu_\pm)\left(\frac{z}{2}\right)^{\nu_\pm}\right] \end{aligned}$$

as $|z|\to 0$. Using this expression, one can identify the terms with r^{-m} and r^m, so one finds A and B. Then the retarded Green's function is found to be

$$G_R(\omega,\vec{k}) = \frac{-\pi e^{-i\pi(m-1/2)}}{sin(\pi(m-1/2))[\Gamma(m+1/2)]^2}\frac{\omega+\vec{k}\cdot\vec{\sigma}}{q}\left(\frac{q}{2}\right)^{2m}. \tag{3.23}$$

The spectral function is given by $A(k,\omega) = -\frac{1}{\pi}Im(Tr(G_R))$. One can see that, as for the bosonic case, the pure AdS background corresponds to the spectral distribution that grows

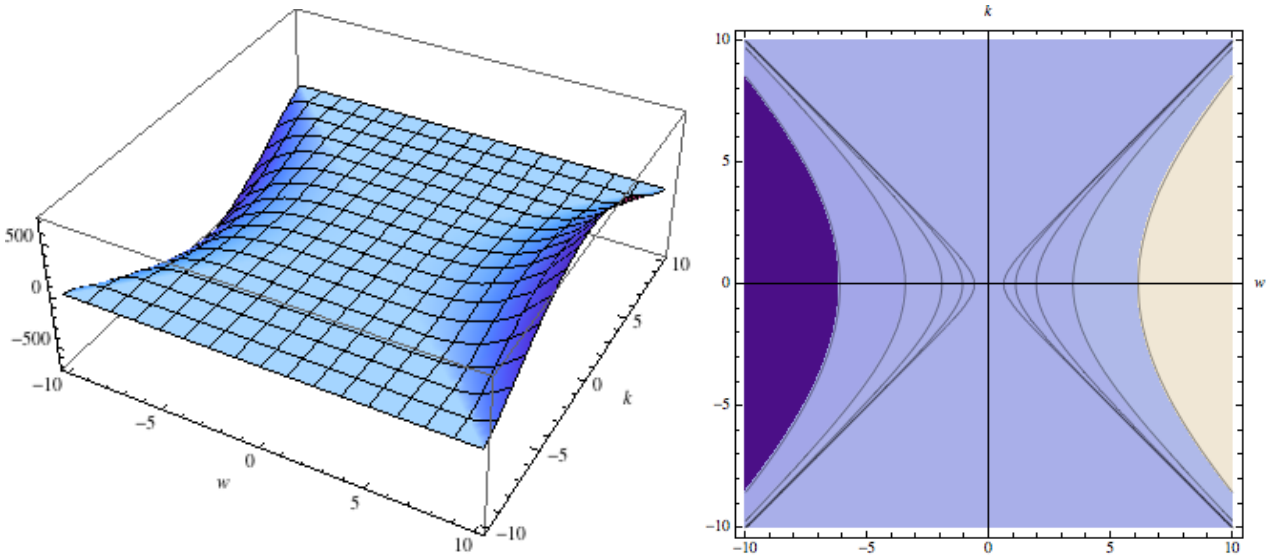

Figure 3.1 The exact spectral function $\chi(\omega, k) = -\frac{1}{\pi} Im(Tr(G_R))$ constructed from the AdS background for $m = 2$. The contours are drawn at $|A| = 0.01, 0.1, 1, 10, 100$. The slope is polynomial, and there is no exponential suppression.

polynomially in ω from $\omega = |\vec{k}|$ to $\omega = \infty$ (see figure 3.1). It reaches 0 at $\omega = \vec{k}$, as the frequency is confined by the relativistic energy-momentum relation $\omega^2 = \vec{k}^2 + m^2$.

Finally, we note that the spectral function does not exhibit the exponential suppression in the limit $\omega \to 0$.

3.3 Numerical Approximation for the AdS_{n+2} and Lifshitz $z > 1$ Backgrounds

In this section, we outline the procedure to obtain the solution numerically for the Lifshitz $z > 1$ backgrounds. The story is the same for the AdS case except minor modification. We first validate our method by comparing the spectral functions obtained through the numerical method with the exact method for the AdS case. Then we present the result of

the calculation for the imaginary Green's function constructed from the Lifshitz $z = 2, 3, 4$ background and discuss some of its features. With the Lifshitz metric,

$$ds^2 = -\left(\frac{L}{r}\right)^{2z} dt^2 + \left(\frac{L}{r}\right)^2 (d\vec{x}_n^2 + dr^2). \tag{3.24}$$

and the Weyl basis, the Dirac equation assumes the following form.

$$\begin{pmatrix} -\partial_r - m/r & \omega r^{z-1} - \vec{k}\cdot\vec{\sigma} \\ \omega r^{z-1} + \vec{k}\cdot\vec{\sigma} & \partial_r - m/r \end{pmatrix} f(r) = 0, \quad f(r) = \begin{pmatrix} f_a(r) \\ f_b(r) \end{pmatrix} \tag{3.25}$$

We first find the expression of infalling boundary condition. From the Dirac equation (3.25), one can find the limiting form of equation for f_a as

$$(\partial_r^2 - \frac{z-1}{r}\partial_r + \omega^2 r^{2z-2}) f_a(r) = 0. \tag{3.26}$$

With the scaling $f_a \to r^{(z-2)/2} f_a$, the equation transforms to a Schrödinger type equation.

$$(-\partial_r^2 + U(r)) f_a(r) = 0, \quad U(r) = \frac{z}{4r^2} - \omega^2 r^{2z-2} \tag{3.27}$$

Using the WKB approximation, one finds

$$f_a(r) \sim \frac{1}{\sqrt[4]{-U}} exp[\pm i \int dr \sqrt{-U}] \sim \frac{C}{r^{(z-1)/2}} exp[\pm i\omega r^z/z] \tag{3.28}$$

for some constant C. Now by scaling back $r^{(z-2)/2} f_a \to f_a$, we find the infalling wavefunctions near horizon as

$$f_a(r \to \infty) = a e^{i\omega r^z/z}, \quad f_b(r \to \infty) = i a e^{i\omega r^z/z} \tag{3.29}$$

in which f_b is found by plugging f_a into the Dirac's equation and a is an arbitrary constant vector.

Now let us consider the limiting forms of wavefunctions at the boundary, which are found from the Dirac equation as before,

$$f_a(r \to 0) = A r^{-m}(1 + \alpha_1 r + \alpha_2 r^2 + \dots) + B r^{m+1}(1 + \beta_1 r + \beta_2 r^2 + \dots) \tag{3.30}$$

$$f_b(r \to 0) = Cr^{-m+1}(1 + \gamma_1 r + \gamma_2 r^2 + \dots) + Dr^m(1 + \delta_1 r + \delta_2 r^2 + \dots). \tag{3.31}$$

where the coefficients are related as $\vec{\sigma} \cdot \vec{k}(2m+1)B = -\vec{k}^2 D$ and $\vec{\sigma} \cdot \vec{k}(2m-1)C = \vec{k}^2 A$. The Green's function is obtained by identifying A as the source and D as the expectation value. A direct approach to the numerical approximation is to start with the two second order linear differential equations for f_a and f_b obtained from the Dirac equation. Then we impose the infalling boundary condition at the horizon, and integrate numerically from the horizon to the boundary. We match the numerical solutions to the above limiting forms using the appropriate number of higher order terms for accuracy. However, it is not easy to find the coefficient D via this way, since the value of function is dominated by the r^{-m+1} term.

For this reason, we introduce

$$\zeta_+(r) = \frac{f_{b+}}{f_{a+}}, \quad \zeta_-(r) = \frac{f_{b-}}{f_{a-}}, \quad f_a = \begin{pmatrix} f_{a+} \\ f_{a-} \end{pmatrix}, \quad f_b = \begin{pmatrix} f_{b+} \\ f_{b-} \end{pmatrix}. \tag{3.32}$$

Then the horizon boundary condition becomes

$$\zeta_\pm(r \to \infty) = i. \tag{3.33}$$

In the meantime, $\zeta_\pm$ takes the following asymptotic forms near the boundary.

$$\zeta_\pm(r \to 0) = \frac{C_\pm}{A_\pm} r + \frac{D_\pm}{A_\pm} r^{2m} \tag{3.34}$$

where we divided each coefficient into two parts as

$$A = \begin{pmatrix} A_+ \\ A_- \end{pmatrix}, \quad B = \begin{pmatrix} B_+ \\ B_- \end{pmatrix}, \quad C = \begin{pmatrix} C_+ \\ C- \end{pmatrix}, \quad D = \begin{pmatrix} D_+ \\ D_- \end{pmatrix}. \tag{3.35}$$

We already know that A and C are related as $\vec{\sigma} \cdot \vec{k}(2m-1)C = \vec{k}^2 A$. If we use the freedom to choose the direction of momentum to make $\vec{\sigma} \cdot \vec{k}$ to be

$$\vec{\sigma} \cdot \vec{k} = \begin{pmatrix} k & \\ & -k \end{pmatrix}, \quad k = |\vec{k}|, \tag{3.36}$$

then they are related as $(2m-1)C_\pm = \pm kA_\pm$. Therefore the ratio $C_\pm/A_\pm$ is now real, and we can eliminate the first term in (3.34) by taking the imaginary part of it, and obtain the imaginary part of the ratio $D_\pm/A_\pm$. For our purpose, it is enough to know the imaginary part, as the spectral function comes from the imaginary part of the retarded Green's function.

Finally, we need the differential expression for $\zeta_\pm$ to connect the horizon to the boundary. By taking the derivative, one finds

$$\zeta'_\pm = -\zeta_\pm \frac{f'_{a\pm}}{f_{a\pm}} + \frac{f'_{b\pm}}{f_{a\pm}}. \tag{3.37}$$

Using the Dirac's equation (3.25), one can turn this into the differential equation for $\zeta_\pm$.

$$\zeta'_\pm + (\omega r^{z-1} \mp k)\zeta_\pm^2 - \frac{2m}{r}\zeta_\pm + (\omega r^{z-1} \pm k) = 0 \tag{3.38}$$

Finally, with the infalling boundary condition, we integrate $\zeta_\pm$ numerically from the horizon to the boundary, and match the imaginary part of our numerical solution to the asymptotic form at the boundary (3.34) to find $Im[D_\pm/A_\pm]$. Then the imaginary part of the retarded Green's function is given by

$$Im[G_R] = Im[-iS\gamma^t] = \begin{pmatrix} Im[D_+/A_+] & \\ & Im[D_-/A_-] \end{pmatrix}, \tag{3.39}$$

and the spectral function is obtained from $\chi(k,\omega) = -\frac{1}{\pi} Im(Tr(G_R))$.

With this procedure described so far, we calculated the spectral function from the AdS background (see figure 3.2), and compared the numerical calculation with the exact calculation of previous section. While there existed some errors for the small values of $\omega < 1$, the relative error was small enough to understand the general behavior, and the numerical calculation converged very closely to the exact solution in the most range (see table A.1).

Now let us consider the spectral function constructed numerically from the Lifshitz $z > 1$ background. The general structure is the same as that from the pure AdS background.

That is, it grows with increasing ω and decline with increasing k with the power law (see figure 3.3 and 3.4), as predicted from the scale invariance of the metric. On the other hand, the spectral function shows the two features that differs from those of the relativistic case.

1. When the spectral function is small (around $A(\omega, k) \sim 1$), its contour line resembles $\omega = k^2/2m$, which is the non-relativistic energy-momentum relation (see figure 3.3).

2. When ω is smaller than $k^2/2m$, the spectral function gets suppressed exponentially. The exponent α in the suppression factor $e^{-\alpha}$, which is found from fitting (see figure 3.5 and table 3.1), is very close to twice that of the spectral function in the bosonic theory. In the bosonic case, the factor was derived as the formula (2.45) using the WKB approximation. From that formula, α for the fermionic case is obtained as

$$\alpha = \begin{cases} \frac{\pi}{2}\frac{k^2}{\omega} & \text{for } z = 2 \\ \frac{\sqrt{\pi}}{3}\frac{\Gamma(1/4)}{\Gamma(3/4)}\sqrt{\frac{k^3}{\omega}} & \text{for } z = 3 \\ \frac{\sqrt{\pi}}{4}\frac{\Gamma(1/6)}{\Gamma(2/3)}\sqrt[3]{\frac{k^4}{\omega}} & \text{for } z = 4 \end{cases} \tag{3.40}$$

First, we note that the dependence of α on the k^z/ω, which is consistent with scale invariance of the metric. In addition, it is interesting that not only both of the spectral functions for bosons and fermions exhibits the exponential suppression in certain regions of momentum space ($\omega \ll 1$, $k \gg 1$), but also the exponent of the factor only differs by 2. While we do not have an explanation at this moment, we expect that the pattern also can be understood in the same way that the bosonic case was explained, that is, in terms of the tunneling barrier and the WKB approximation near boundary.

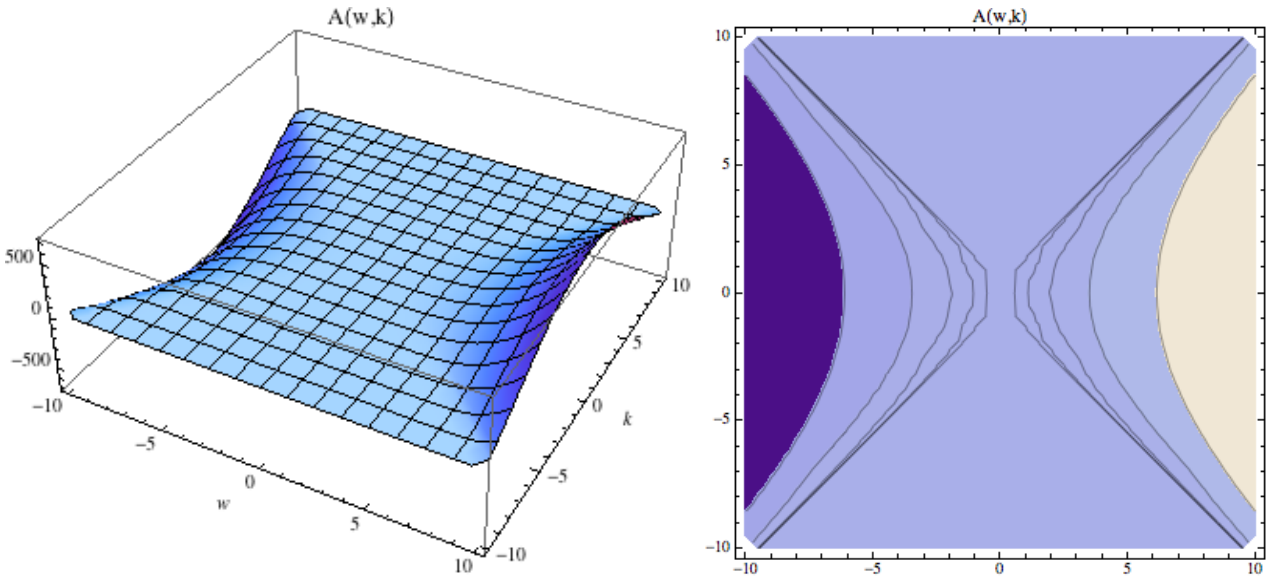

Figure 3.2 The spectral function $\chi(w, k)$ obtained numerically from the AdS background.

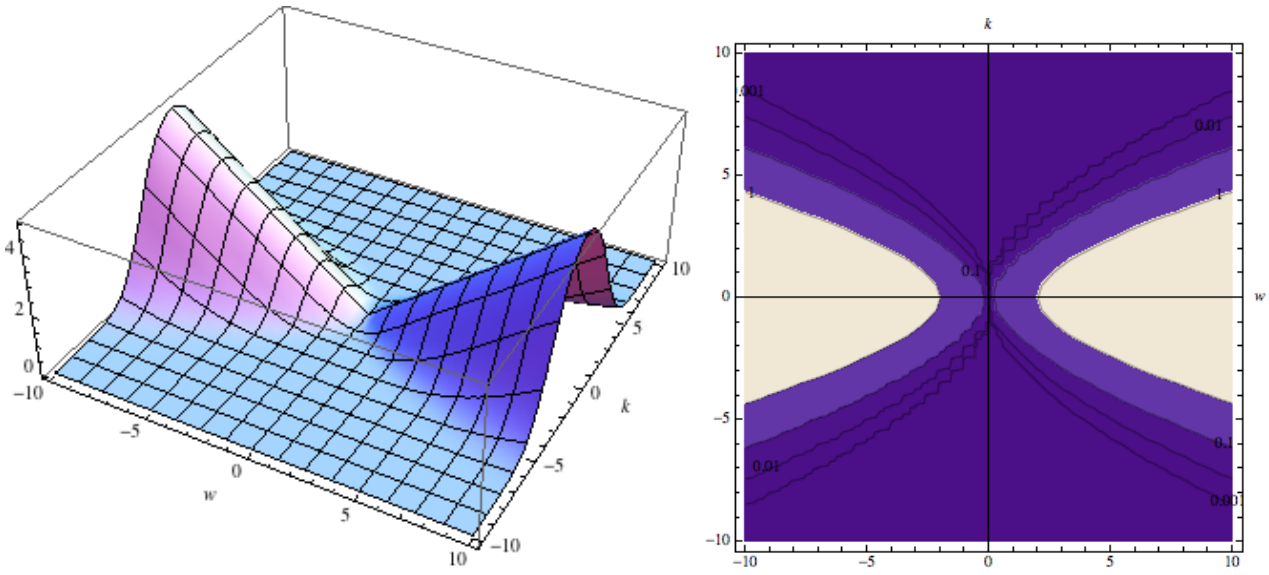

Figure 3.3 The spectral function $\chi(w, k)$ obtained numerically from the Lifshitz $z = 2$ background for $m = 1$. The contour lines are drawn at $\chi(\omega, k) = 0.001, 0.01, 0.1, 1$. One can see that the contour line approaches $\omega = k^2/2m$ near $\chi(\omega, k) = 1$, and $\chi(\omega, k)$ decreases exponentially beyond this line.

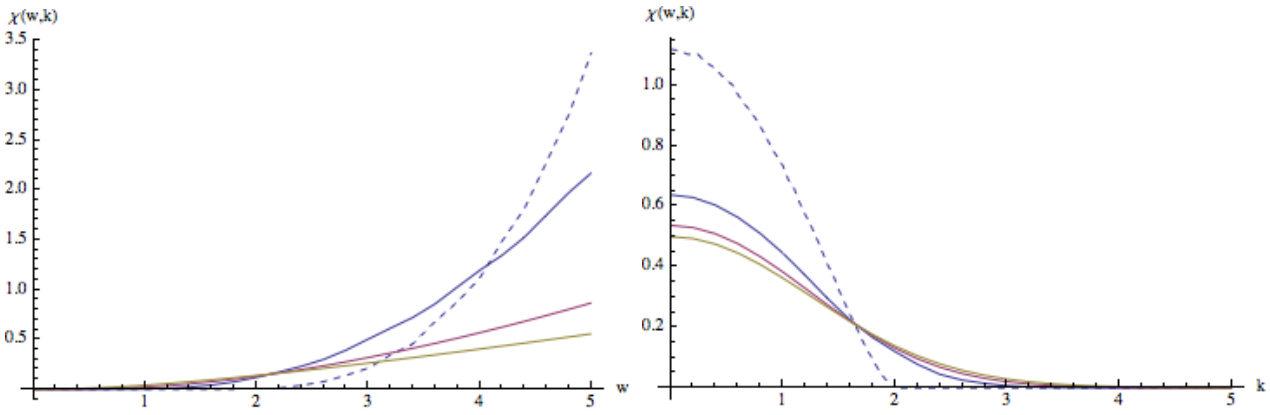

Figure 3.4 The holographic spectral function calculated numerically from the AdS (dashed) and the Lifshitz $z = 2, 3, 4$ (blue, red, green) backgrounds for $k = 2$ (left plot) or $\omega = 2$ (right plot) with $m = 2$. We set the normalization constant $K = 1$ except for the AdS case with fixed k, where $K = 0.1$.

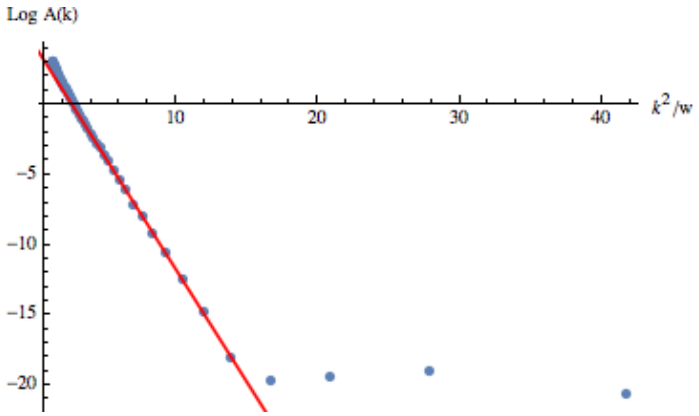

Figure 3.5 The values of spectral function $Log\chi(\omega, k)$ obtained numerically from the Lifshitz $z = 2$ background for $m = 2$ and $k = 5$. The red line is the result of fit of $\alpha_0(k^2/\omega)+constant$ in the region $\omega < k^2/2m$. For this case, $\alpha_0 = 1.6038$. We ignored the points where ω is so small that the numerical result is not reliable.

$z = 2$	$z = 3$	$z = 4$
$\alpha_2 \frac{k^2}{\omega}$	$\alpha_3 \sqrt[2]{\frac{k^3}{\omega}}$	$\alpha_4 \sqrt[3]{\frac{k^4}{\omega}}$

m	k	α_2	α_3	α_4
1	3	1.5935	1.7875	1.8691
1	5	1.5917	1.7715	1.8405
1	7	1.5824	1.7510	1.8287
2	3	1.5941	1.8533	1.9655
2	5	1.6038	1.8175	1.8813
2	7	1.5977	1.7993	1.8453
3	3	1.5968	1.9975	2.0830
3	5	1.6006	1.8806	1.9167
3	7	1.5855	1.8575	1.8334
$2\alpha_{i,\mathrm{WKB}}$		1.5707	1.7480	1.8214

Table 3.1 The exponents of the exponential factors in the spectral function from the Lifshitz $z = 2, 3, 4$ background with fermions (left table) and the constant α_i in the exponent (right table) in the limit $\omega \ll 1$, $k \gg 1$. They were obtained by fitting the exponents to $\log \chi(\omega, k)$ in the region $\omega < k^2/2m$. The last row is twice the constant in the exponent of exponential factor in the spectral function from bosonic AdS/CFT.

Chapter 4

Discussion

The main motivation of our study was to answer whether the holographic Green's function constructed from the Lifshitz spacetime and fermions exibits the exponential insensitivity to the horizon boundary condition that was found using AdS/CFT with bosons in the certain region of momentum space $\omega \ll 1, k \gg 1$. This insensitivity was manifested in the exponential vanishing of the spectral function in this region of momentum space. We found that the answer is yes, that is, the spectral function shows the exponential suppression in the low energy, large momemtum limit in the fermionic AdS/CFT, and the expression for the exponential factor for each z carries over from the bosonic cases with the additional constant factor. This is an interesting result considering the difference in the ways that scalars and spinors couple to the curved spacetime.

As the fermions have more relevance to realistic condensed matter systems, our finding may open the possibility to make connection between this duality and experiments. Since the spectral function can be the measure for the density of states, it also can be used to calculate transport coefficients such as thermal and electrical conductivities. Therefore the universal behavior of spectral function in the low energy, large momentum limit for the Lifshitz background can lead to universal predictions in the corresponding field theories.

It is also interesting to consider how this insensitivity may rescue AdS/CFT with the Lifshitz geometry. It has been shown that the Lifshitz geometry suffers from a naked singularity at the horizon, which lead to unphysical results [19]. Various mechanisms to resolve the singularity were introduced, which lead to different near horizon geometries. Our finding solidifies the previous notion that the field theory may care little about how the Lifshitz horizon is resolved [12]. The argument is that the geometric resolution at the horizon leads to introducing a low-energy regulator, but this only gives an exponentially small correction to the boundary Green's function, as it becomes insensitive to the horizon geometry in the low energy, large momentum limit.

What is lacking in our analysis is the explanation of this exponential decoupling. For AdS/CFT with scalars, it was possible to find the exact Green's function for the Lifshitz $z = 2$ case, and examine its limiting behavior. In addition, we had a more intuitive picture in terms of the effective potential and the WKB approximation. It was the region of potential falling slower than $\sim 1/r^2$ that introduced the decay of amplitudes containing the horizon boundary condition. We leave the search of exact boundary Green's function and the WKB approximation for the spinors in the Lifshitz geometry as future study.

Appendix A

Appendices

A.1 The Green's Function and the Spectral Distribution

In this section, the relation between the Green's function and the spectral distribution will be discussed. The Green's function allows to represent the solution of a differential equation in terms of an integral and a source term. The Green's function can be expressed in momentum space by the Fourier transform. Assuming the source is concentrated at $y^\mu = 0$

$$G(x^\mu) = \int \hat{G}(k^\mu) e^{-ik_\alpha x^\alpha} \frac{d^4k}{(2\pi)^4}, \tag{A.1}$$

where $k^\alpha = (w, \vec{k})$. Then $\Box\hat{G}(k^\mu) = 1$, and also $\Box\hat{G}(k^\mu) = -k_\alpha k^\alpha \hat{G}(k^\mu)$. Therefore the Green's function in momentum space and in coordinate space are related by

$$\hat{G}(k^\mu) = \frac{1}{w^2 - |\vec{k}|^2}, \tag{A.2}$$

$$G(x^\mu) = \int \frac{e^{-i(\vec{k}\cdot\vec{x} - \omega t)}}{\omega^2 - |\vec{k}|^2} \frac{d\omega d^3\vec{k}}{(2\pi)^4}, \tag{A.3}$$

This integral can be calculated through the contour integral with displaced poles.

$$G(x^\mu) = \int \frac{e^{-i(\vec{k}\cdot\vec{x} - \omega t)}}{(\omega + i\epsilon)^2 - |\vec{k}|^2} \frac{d\omega d^3\vec{k}}{(2\pi)^4}, \tag{A.4}$$

It can be shown that $G(x^\nu) = 0$ for $t < 0$, and for $t > 0$,

$$G(x^\mu) = \frac{\delta(r - ct)}{4\pi r}. \tag{A.5}$$

This is the manifestation of the field propagating at the speed of light. In the momentum space, the Green's function gives the information on the dispersion relation. By expanding the Green's function in the complex plane, one finds

$$\hat{G}(k^\mu) = \frac{1}{\omega^2 - k^2 + \epsilon^2} - \frac{2i\omega\epsilon}{(\omega^2 - k^2 + \epsilon^2)^2}. \tag{A.6}$$

Therefore the imaginary part of the Green's function tells us the dispersion relation for the particle, and in this case $\omega = \pm k$. Hence from the distribution of the imaginary part of the Green's function, we are able to obtain the spectrum of dispersion relations corresponding to the quasi-particles.

	$k=2$			$k=5$		
ω	χexact	χnum.	res. (%)	χexact	χnum	res. (%)
0.5	0.0044209	0.0053435	-20.87	0	0	
1	0.070735	0.066246	6.35	0	0	
1.5	0.35809	0.28801	19.57	0	0	
2	1.1317	1.1546	-2.02	0	0	
2.5	2.7631	2.2452	18.74	0	0	
3	5.7295	5.3148	7.24	0	0	
3.5	10.614	10.148	4.39	0	0	
4	18.108	17.742	2.02	0	0	
4.5	29.006	28.853	0.53	0	0	
5	44.209	44.033	0.40	0	0	
5.5	64.727	64.554	0.27	4.679	4.3325	7.41
6	91.673	91.331	0.37	15.483	15.416	0.43
6.5	126.26	125.73	0.42	32.940	32.737	0.62
7	169.83	168.98	0.50	58.217	57.914	0.52
7.5	223.81	222.39	0.63	92.677	92.527	0.16
8	289.73	287.82	0.66	137.82	136.95	0.63
8.5	369.24	366.70	0.69	195.28	194.27	0.52
9	464.09	460.93	0.68	266.78	265.34	0.54
9.5	576.14	572.44	0.64	354.18	354.05	0.04
10	707.35	703.01	0.61	459.44	460.22	-0.17

Table A.1 The values of spectral functions $\chi_{\text{exact}}(\omega, k)$ and $\chi_{\text{num.}}(\omega, k)$ calculated exactly and numerically from the AdS spacetime using fermionic AdS/CFT, where the normalization constant was set to be $K = 1$. The 4th and 7th columns are the residual errors of numerical values as the percentage of exact value.

Bibliography

[1] J. D. Bekenstein, *"Black Holes and Endtropy"*, Phys. Rev. **D7** (1973) 2333.

[2] R. Bousso, *"The holographic principle"*, Rev. Mod. Phys. **74** (2002) 825, arXiv:hep-th/0203101

[3] J.M. Maldacena, *"The Large N Limit of Superconformal Field Theories and Supergravity"*, Adv. Theor. Math. Phys. **2** (1998) 231.

[4] S. Kachru, X. Liu and M. Mulligan, *"Gravity duals of Lifshitz-like fixed points,"* Phys. Rev. D **78**, 106005 (2008) arXiv:0808.1725 [hep-th].

[5] C. Charmousis, B. Gouteraux, B. S. Kim, E. Kiritsis and R. Meyer, *"Effective Holographic Theories for low-temperature condensed matter systems,"* JHEP **1011**, 151 (2010) arXiv:1005.4690 [hep-th].

[6] D. T. Son, *"Toward an AdS/cold atoms correspondence: A Geometric realization of the Schrodinger symmetry,"* Phys. Rev. D **78**, 046003 (2008) arXiv:0804.3972 [hep-th].

[7] K. Balasubramanian and J. McGreevy, *"Gravity duals for non-relativistic CFTs,"* Phys. Rev. Lett. **101**, 061601 (2008) [arXiv:0804.4053 [hep-th]].

[8] S. A. Hartnoll, *"Lectures on holographic methods for condensed matter physics"*, Class. Quant. Grav. **26** (2009) 224002, arXiv:0903.3246 [hep-th].

[9] S. Sachdev, *"Condensed Matter and AdS/CFT,'* Lect. Notes Phys. **828**, 273 (2011) arXiv:1002.2947 [hep-th].

[10] D. T. Son and A. O. Starinets, *"Minkowski space correlators in AdS / CFT correspondence: Recipe and applications"*, JHEP **0209** (2002) 042, arXiv:hep-th/0205051 [hep-th].

[11] C. Keeler, G. Knodel, and J. T. Liu, *"What do non-relativistic CFTs tell us about Lifshitz spacetimes"*, arXiv:1308.5689 [hep-th]

[12] C. Keeler, G. Knodel, and J. T. Liu, *"Hidden horizons in non-relativistic AdS/CFT"*, arXiv:1404.4877 [hep-th]

[13] N. Iqbal and H. Liu, *"Real-time response in AdS/CFT with application to spinors"*, arXiv:0903.2596 [hep-th]

[14] M. Abramowitz and I. A. Stegun, *Handbook of Mathematical Functions: with Formulas, Graphs, and Mathematical Tables*, Dover Publications (1965)

[15] M. Natsuume, *AdS/CFT Duality User Guide*, Springer (2015), arXiv:1409.3575 [hep-th]

[16] M. Alishahiha, M. Mozaffar, and A. Mollabashi, *"Fermions on Lifshitz Background"*, arXiv:1201.1764 [hep-th]

[17] N. Iqbal and H. Liu, *"Real-time response in AdS/CFT with application to spinors,"* Fortsch. Phys. **57**, 367 (2009) arXiv:0903.2596 [hep-th].

[18] D. Z. Freedman and A. Van Proeyen, *Supergravity,* Cambridge, UK: Cambridge Univ. Pr. (2012)

[19] G. T. Horowitz and B. Way, *"Lifshitz Singularities,"* Phys. Rev. D **85**, 046008 (2012) arXiv:1111.1243 [hep-th].